1 CYCLIC DIRECT SIMPLE SHEAR TEST TO MEASURE STRAIN-

2 DEPENDENT DYNAMIC PROPERTIES OF UNSATURATED SAND

- **Khoa N. Le**, Graduate Research Assistant, Department of Civil and Environmental
- 4 Engineering, University of New Hampshire Durham, USA,
- 5 <u>knf8@wildcats.unh.edu</u>
- **Majid Ghayoomi**, Ph.D., Assistant Professor, Department of Civil and Environmental
- 7 Engineering, University of New Hampshire Durham, USA,
- 8 <u>majid.ghayoomi@unh.edu</u>

ABSTRACT:

The dynamic properties of a clean sand under different degrees of saturation is investigated using a modified custom built Direct Simple Shear (DSS) apparatus at the University of New Hampshire. The specific characteristics of the DSS are presented and the testing procedures are discussed. The device utilizes the axis translation and tensiometric techniques to control the matric suction in the soil specimen. The investigation on F75 Ottawa Sand shows a decrease in shear modulus and an increase in damping by increasing the shear strain over the tested range of strains for various degrees of saturation; dry, saturated, and partially saturated. The modulus reduction in the applied range of medium shear strains regardless of the degree of saturation demonstrates the capability of the DSS in consistently capturing the changes of dynamic properties. Experimental results indicate that the matric suction can have a substantial effect on the stiffness of the soil. However, the extent of this effect may depend on the induced strain level the effective stress in unsaturated soil. In addition, partially saturated specimens resulted in lower dynamic compression.

KEYWORDS: direct simple shear, unsaturated soil, shear modulus, damping ratio

INTRODUCTION

26

27

28

29

30

31

32

33

34

35

36

37

38

39

40

41

42

43

44

45

46

47

48

49

The behavior of dynamically loaded soils has been a topic of interest to geotechnical engineers. In order to understand this behavior, key dynamic soil parameters such as shear modulus (G) and damping ratio (Z) have been studied in both laboratory (e.g. using acoustical methods, dynamic triaxial, resonant column, direct simple shear) and in-situ settings (e.g. using seismic techniques, penetration tests) (Kramer 1996). These parameters are critical when analyzing geotechnical sites and structures subjected to seismic motions. Stress state, effective confining pressure, soil mineralogy, density, and induced shear strain are the main factors affecting these dynamic parameters. For example, the shear modulus degrades nonlinearly by increasing the shear strain level whereas the shear modulus at small shear strains (i.e. $y < 10^{-4} \sim 10^{-2}\%$) is often referenced to as the maximum shear modulus (G_{max}). Damping ratio, however, follows a reverse trend as the shear strain increases. In recent years, theoretical and experimental advancements in understanding the behavior of unsaturated soils has revealed the importance of the degree of saturation on the shear modulus and damping in geomaterial. Small-strain moduli (.0001% – 0.01%) of various soils under different degrees of saturation using the resonant column and bender element tests have been extensively investigated and several empirical relations were proposed (Wu et al. 1984, Qian et al. 1991, Marinho et al. 1995, Mancuso et al. 2002, Matesic and Vucetic 2003, Mendoza et al. 2005, Ng et al. 2009, Khosravi et al. 2010, Khosravi and McCartney 2011, Ghayoomi and McCartney 2011, Kumar and Madhusudhan 2012, Hoyos et al. 2015). These studies denoted a higher shear modulus and lower damping in partially saturated soils due to the presence of inter-particle suction stresses that increase the soil stiffness. Results by Qian et al. (1984) and Ghayoomi and McCartney (2011) indicated a general increase in small-strain shear modulus of sands up to a peak value before the residual water content. However, a continuous rise of modulus was reported by Khosravi and McCartney (2011) as suction increases in silty material. In addition, results of this study revealed a hysteresis behavior in G_{max} values along the drying and wetting paths of Soil-Water Retention Curve; a behavior which have been postulated to be due to plastic hardening during drying. Hoyos et al. (2015) observed the same trend for a silty sand, in which, also, the damping decreased by increasing the suction. Further, Michaels (2006) performed viscoelastic analyses to estimate viscous damping in partially saturated soils and verified the results with field measurements. He concluded that higher degrees of saturation lead to higher damping ratios for the same excitation frequency.

At medium shear strain levels (0.01% - 0.1%), modifications were made to triaxial systems to incorporate suction control to study the dynamic properties of unsaturated soils (Cui et al. 2007, Chin et al. 2010, Craciun and Lo 2010, Biglari et al. 2011, Kimoto et al. 2011, Ghayoomi et al. 2016). These studies indicated an increase in stiffness of unsaturated soils in higher suction following a strain-dependent modulus reduction pattern similar to the ones in dry condition. However, difficulties in converting Young's modulus and axial strain to shear modulus and shear strain and accurately measuring volumetric strain hindered their use in estimating shear modulus of unsaturated soils. Further, the medium to large strain (> 0.1%) dynamic properties have also been examined using direct simple shear apparatuses (Jafarzadeh and Sadeghi 2011, Milatz and Grabe 2015), but the shear modulus results were not well presented and deeply discussed. In general, despite the extensive effort in characterizing and formulating the small-strain modulus and damping of unsaturated soils, the extent of the work on the response of

unsaturated soils in medium to large strain have been very limited. By synthesizing the lessons learned from the response of dynamically loaded soils and the dynamic properties of unsaturated soils, geotechnical engineers can better predict the seismic behavior of geotechnical systems, especially when these systems are within the phreatic zone. Therefore, a more accurate assessment and more sustainable and cost-effective geotechnical design would be acquired.

Further, the dynamic compression of soils is important in evaluating the seismically induced settlement of foundations or embankment fills. Recently, researchers investigated the dynamic compression of compacted unsaturated soils in the laboratory by varying applied shear strain, stress history, effective confining stress, soil type, and water content using cyclic Direct Dimple Shear (DSS) test (e.g. Whang et al. 2004, Hsu and Vucetic 2004, Duku et al. 2008). However, these studies were not performed under suction-controlled setting, except the work by Ghayoomi et al. (2013) who looked at the seismically induced settlement of partially saturated soil layers inside the geotechnical centrifuge. Therefore, further research is needed to characterize the dynamic properties and dynamic compression of partially saturated soils subjected to medium to large shear strains in a suction-controlled laboratory environment. The DSS is a unique piece of laboratory equipment that can be employed to serve both purposes (i.e. determining dynamic properties while simultaneously controlling matric suction and measuring the dynamic compression), although it requires preliminary verification and quality control.

This paper focuses on the modification, calibration, and implementation of a custom built direct simple shear apparatus (Miller 1994, Dunstan 1998) in order to control suction and study the effects of degree of saturation and applied shear strain on the shear modulus and damping. Background theory on dynamic properties and unsaturated soil

mechanics are briefly discussed followed by the apparatus description, modifications to the machine, experimental procedures, and data reduction methods. The effects of the degree of water saturation (e.g. dry, fully saturated, and partially saturated conditions) of a sandy material on shear modulus, damping, and dynamic compression are discussed. The degradation of the shear modulus over a small range of medium shear strains is presented and system performance is verified. Ultimately, the extent to which suction influences the shear modulus is discussed by isolating the effect of the mean effective stress. The goals of this paper are threefold: 1) Discuss the characteristics of a custombuilt DSS capable of controlling suction; 2) Validate the consistent performance of the DSS over a range of strain and suction levels; 3) Evaluate the extent to which suction affects shear modulus of unsaturated soils.

BACKGROUND

Dynamic Shear Modulus and Damping

Previous investigations have indicated that the shear modulus is based on key material and state parameters such as the void ratio (e), effective mean confining stress (σ'_m), stress history, applied shear strain, and soil type (Kramer 1996). For example, Seed and Idriss (1970) compiled data from resonant column, forced vibration, and torsional shear tests on sand to develop the following formula for small strain shear modulus.

$$G_{max} = 1000K_{2,max}(\sigma'_m)^{1/2} \tag{1}$$

where $K_{2,max}$ is a function of the relative density and σ'_m is the effective mean confining pressure. Since then several other equations have been proposed to capture the small strain modulus, including the equations that incorporate suction or degree of saturation (e.g. Hoyos et al. 2015).

The strain-dependent shear modulus represents the soil stiffness for a given shear strain. The value is obtained by interpreting data from the non-linear shear stress – strain response of soils under cyclic load that typically follows hysteresis loops shown in Figure 1. The stiffness of the soil can be determined by estimating the secant shear modulus as the slope of the hysteresis loop from the origin to the point of interest,

$$G_{sec} = \frac{\tau}{\gamma} \tag{2}$$

where G_{sec} (or G) represents the shear modulus, τ is shear stress, and γ represents the corresponding shear strain. An empirical formula for the strain dependent shear modulus by Seed and Idriss (1970) in Equation 3 takes on a similar syntax to Equation 2, substituting G_{max} for G and K_{2max} with K_2 which instead is a function of both relative density and the degradation ratio parameter, i.e. G/G_{max} , as in Equation 4,

$$G = 1000K_2(\sigma_m')^{1/2} \tag{3}$$

The degradation of the shear modulus over a range of strains was presented using a shear modulus reduction function by Hardin and Drnevich (1972). They normalized the shear modulus measured at a particular strain over the maximum shear modulus and formulated it via a hyperbolic function in the form shown Figure 2. Darendeli (2001) and Menq (2003) proposed a modified hyperbolic function based on the results of numerous resonant column and torsional shear tests. Oztoprak and Bolton (2013) compiled a database of modulus measurements for various soils and testing conditions and incorporated the modified framework by Menq (2003). They used a multivariable regression model to depict the best relationship for estimating the fitting parameters shown in Equation 4.

$$\frac{G}{G_{max}} = \frac{1}{\left[1 + \left(\frac{\gamma - \gamma_e}{\gamma_r}\right)^a\right]}$$

$$\gamma_r (\%) = 0.01C_u^{-0.3} \left(\frac{\sigma'_m}{P_{atm}}\right) + 0.08eD_r$$

$$\gamma_e = 0.0002 + 0.012\gamma_r$$

$$a = C_u^{-0.075}$$
(4)

where γ is the shear strain, and γ_r is the reference shear strain corresponding to $G/G_{max}=0.5$, γ_e is the elastic threshold shear strain, P_{atm} is atmospheric pressure, e is void ratio, and D_r is the relative density, a is a curvature parameter a, and C_u is the coefficient of uniformity.

Damping ratio represents the amount of energy that is dissipated by the soil when subjected to dynamic loading. The strain-dependent trends in damping ratio (ζ) and shear modulus are often reciprocal whereas the shear modulus degrades while the damping ratio increases; for example in a simple form as in Equation 5 (Hardin and Drnevich 1972) or in more complex forms as in Equation 6.

$$\frac{\zeta}{\zeta_{max}} = 1 - \frac{G}{G_{max}} \tag{5}$$

$$\zeta = b \left(\frac{G}{G_{max}} \right)^{0.1} * \zeta_{masing} + \zeta_{min}$$
 (6)

where ζ is the damping ratio, ζ_{min} is the minimum or small-strain damping ratio, ζ_{max} is the maximum damping ratio, ζ_{masing} is a modified form of damping based on "Masing behavior", and b is a scaling coefficient (based on the cycle number) for the ζ_{masing} response. "Masing behavior" relates the soils' monotonic loading response (via the backbone curve) with the cyclic unloading and reloading response (Masing 1926, Darendeli 2001).

Examining the abovementioned empirical equations, one would clearly see that the direct effect of degree of saturation (suction) on the dynamic soil parameters is neglected. Although the data might have been obtained from wet unsaturated soils, no direct control of suction was involved. In addition, consequences of changes in degree of saturation was not evaluated and discussed. Despite the previous effort to formulate suction-dependent small strain modulus, the suction-dependency of strain-dependent modulus received less attention.

Effective Stress in Unsaturated Soils

In classical soil mechanics, effective stress is a fundamental component of many mechanical soil properties as explained by Terzaghi (1943) and modified by Bishop (1959) for a range of degrees of saturation shown in Equation 7.

$$\sigma' = (\sigma - u_a) + \chi(u_a - u_w) \tag{7}$$

In this equation, $(\sigma - u_a)$ represents the net normal stress, $(u_a - u_w)$ is the matric suction, and χ is Bishop's effective stress parameter. The effective stress parameter is often a function of the degree of saturation; the value is zero, when referencing a dry soil and 1, when referencing a fully saturated soil. Different approaches have been introduced to estimate the effective stress parameter. Lu et al. (2006) introduced suction stress as a product of the effective stress parameter and suction to calculate induced additional "tensile" strength into the soil matrix. Using this concept, Lu et al. (2010) incorporated the van Genuchten (1980) Soil-Water Retention Curve (SWRC) model fitting parameters into Bishop's equation to estimate the effective stress in unsaturated soils, as in Equation 8.

$$\sigma' = \sigma - u_a + \frac{u_a - u_w}{(1 + [\alpha(u_a - u_w)]^n)^{1 - \frac{1}{n}}}$$
(8)

where α and n are van Genuchten SWRC parameters. An alternative method to determine the effective stress parameter was proposed by Khalili and Khabbaz (1998) where χ parameter takes form through the following piecewise function where $(u_a-u_w)_b$ is the soil air entry value in SWRC (Equation 9).

$$\chi = \left(\frac{u_a - u_w}{(u_a - u_w)_b}\right)^{-0.55} \qquad u_a - u_w > (u_a - u_w)_b$$

$$\chi = 1 \qquad u_a - u_w \le (u_a - u_w)_b$$
(9)

Many mechanical properties of soils including dynamic modulus and damping ratio are influenced by the effective stress in the soil. Incorporating the effects of degree of saturation and inter-particle suction in the effective stress using relations such as Equations 8 and 9, has been one common approach to estimate soil characteristics. As a result, developing empirical, effective stress-based relations for dynamic soil properties consistent for various degrees of saturation would streamline the seismic analysis of geosystems in unsaturated soils. However, such relations need to be verified using experimental data before their application. For example, Ghayoomi and McCartney (2011) combined the results from bender element and resonant column tests on dry, saturated, and unsaturated sands and proposed a consistent formula for small-strain shear modulus regardless of the degree of saturation given the modified effective stress equation. However, recent work by Ghayoomi et al. (2016) indicated that a modified effective stress-based formula may still not fully capture the suction dependency of soil dynamic properties. On the other hand, Dong et al. (2016) argued that the water-soil

matrix interface friction can be reduced in unsaturated soils that would lead to softer soil as opposed to the stiffening in presence of suction.

The Cyclic Direct Simple Shear (Cyclic - DSS) test is an element level experiment used

TESTING SYSTEMS

194

195

196

197

198

199

200

201

202

203

204

205

206

207

208

209

210

211

212

213

214

215

216

217

Cyclic Direct Simple Shear Apparatus

to characterize dynamic properties of soils including shear modulus, damping, and dynamic compression. Although there are numerous tests to determine the dynamic properties of soils both in laboratory and in the field DSS test is one of the geomechanically preferred methods due to the direct measurement of shear stress and strain. It replicates the response of an element of soil inside a soil column under a dynamic shear motion where shear wave propagates upward. A soil specimen is confined inside a flexible boundary to reduce the boundary effects. In addition, selecting a low height to diameter ratio will improve the uniformity of shear strain distribution along the specimen (Shen et al. 1978). Over the last century, several versions of this machine have been built and tested while they differed in loading mechanism, specimen confinement method, instrumentation, and specimen sizes (Kjellman, 1951, Budhu 1984, Airey and Wood 1987). A custom built Direct Simple Shear (DSS) system developed at the University of New Hampshire was originally designed and created to perform cyclic shear or other dynamic displacement-controlled tests (Miller 1994, Dunstan 1998). This system has been recently renovated and re-operated by upgrading the motion controller and measurement sensors (Le 2016). The DSS framework consists of a steel reaction frame and utilizes two sets of high capacity – low friction Thomson roller slides to provide movement in the vertical and horizontal direction. The DSS accommodates cylindrical soil samples that are 1 in

(2.54 cm) in height and 4 in (10.16 cm) in diameter with a height-to-diameter ratio of 0.25; less than 0.4 as recommended by ASTM D6528. The soil cell is based off of the Swedish Geotechnical Institute (SGI) configuration (Kjellman 1951) by using a stack of Teflon coated aluminum rings to impose the lateral confinement around the sample. A manual pneumatic piston is used to control the loading in the vertical direction, while a hydraulic actuator incorporated into a Proportional-Integral-Derivative (PID) servovalve loop (using a capacitance transducer as feedback) is used to allow dynamic loading in the horizontal direction.

218

219

220

221

222

223

224

225

226

227

228

229

230

231

232

233

234

235

236

237

238

239

240

241

In this project, a sinusoidal wave function was generated by setting the amplitude, frequency, and number of cycles through a NI LABVIEW program. The signal was then transformed from an electric signal to a mechanical movement by means of a MOOG amplifier and servo-valve. The servo-valve controls the movement of fluid flow entering and exiting the hydraulically pressurized actuator to provide a horizontal movement to the system. The movement is then transferred to a damper system which contains a steel beam and a set of springs to stabilize the imparted motion to the soil chamber. These springs also allow for different ranges of motion to be achieved. The transferred motion is recorded by a horizontal load cell before it reaches the bottom table of the soil chamber. A MTI Instruments ASP-500M-CTA capacitance transducer with a measurement resolution of 30 nm is placed on the other side of the soil chamber that provides a horizontal displacement reading. The reading is then sent back to controller and the control loop continues until the conditions of the signal (i.e. duration and displacement) are reached. Various sensors including the horizontal capacitive transducers, a high resolution Sensotec PLVX vertical LVDT, an Interface SSM-AJ-250 horizontal load cell and an Interface 1500ASK-300 vertical load cell are used to capture the response of the soil sample including horizontal and vertical displacement and load. The architectural schematic and an inclusive picture of the system are shown in Figures 3 and 4, respectively. The current DSS setup allows users to tests samples with imparted cyclic strains at 0.02% and higher. The current investigation is focused on medium strain levels (ie. 0.02% - 0.059%). However, by changing the horizontal spring set-up with different stiffness lower or higher shear strains would be achieved.

Suction Control System

242

243

244

245

246

247

248

249

250

251

252

253

254

255

256

257

258

259

260

261

262

263

264

265

In order to introduce and control the matric suction in the soil sample, the system was modified to enable axis translation technique proposed by Hilf (1956). The technique uses an enclosed soil chamber with a medium that can separate the air-water interface. Often, this medium is in the form of a High Air Entry Value (HAEV) ceramic disc and allows the flow of water through the disk, while prohibiting the flow of air (past a threshold value). The sample is, then, built on top of the ceramic disk and the air or water pressure is changed to a designated value. However, in the tests presented herein, the air pressure was kept zero while negative water pressure was applied. This would simulate a tensiometric suction control as oppose to standard axis translation where the pore air pressure is typically increased to be greater than the pore water pressure as discussed by Marinho et al. (2008). A reference axis was established at the middle of the sample while the water pressure was lowered so that a decrease in the water pressure below the reference axis would be considered as the matric suction applied to the sample. It should be noted that it often takes an extended period of time to allow equilibrium to occur within the soil matrix. Considering the independent control of air and water pressure in the specimen both axis translation and tensiometric approaches are practicable using this system.

The DSS at UNH utilizes a HAEV disk rated at ½ bar (50 kPa) that is embedded into the bottom platen of the soil chamber. The platen below the disk contains a grooved channel connected to water lines that allow the disk to be flushed out if any entrapped air bubbles are present in the lines. Additional hydraulic lines are also used to connect a flowpump to the bottom of the sample. The Geotac Digiflow pump used in this machine has a reservoir capacity of 4.58 in³ (75 mL) and is capable of applying pressures of up 300 psi (2068 kPa). It is also fitted with a pressure sensor of 100 psi (690 kPa) to provide feedback to the Geotac software. Similar to the PID system that is integrated in controlling the horizontal actuator, the pump is controlled through software and allows users to control the pressure, flow-rate, or volume of water in the soil system and uses various sensors to maintain constant pressures when dynamic loading is in progress. The PID system in the flow pump system allows the soil sample to reach a steady state condition with negligible flow of water. Although the pump is capable of applying large pressure, it is limited to 7.25 psi (50 kPa) due to the limits of the HAEV disk. In addition, a Validyne Differential Pressure Transducer (DPT) rated at 14.5 psi (100 kPa) with 0.1% full span resolution was used to independently measure the differential pressure between atmospheric air pressure and the pore water pressure (i.e. suction) in the sample. Prior to testing, the DPT was also used to establish the reference pressure that was associated with the reference axis. During the tests, the DPT provided real time water pressure measurements in the sample. A closer view schematic of the DSS soil chamber is shown in Figure 5.

286

266

267

268

269

270

271

272

273

274

275

276

277

278

279

280

281

282

283

284

285

287

288

289

PROCEDURES

Material and Testing Methods

The material used for this investigation was F-75 Ottawa sand. It is classified as a clean, poorly graded (SP) silica-based sand. The soil gradation curve can be seen in Figure 6 and a summary of the geotechnical properties are presented in Table 1. Soil specimens were created by assembling the soil chamber mold and using the dry pluviation method to rain the sand into the cell to a relative density of 45%. The soil specimen was then inserted into the DSS apparatus using T-Clamps to attach the bottom and top tables to the chamber. The soil was compressed through the use of the pneumatic actuator and regulator to a total vertical confining pressure of 7.25 psi (50 kPa). Readings from the vertical load cell and LVDT were recorded. With the exception of the dry specimen, the soil was then saturated by flushing de-aired water through the bottom of the specimen and out from the top of the soil specimens. The specimen was kept soaked in the water for a few hours to maintain the saturated condition. Specimens that were to be tested under partially saturated conditions were then desaturated to the target matric suction level using the abovementioned tensiometric technique.

SWRC was obtained by constructing a soil sample in the DSS soil chamber, fully saturating, and then incrementally desaturating the sample. The water pressure below the disk was decreased at increments of approximately 1 kPa, while the air pressure at the top of the sample was left open to the atmosphere. Readings of the volume of water extracted from the sample were taken from the Geotac software. Once the flow of water from the bottom of the sample was steadily less than 0.002 mL/min, the soil matrix was considered to be under equilibrium. The SWRC that was established is shown in Figure 7 and compared with previous results for the same soil. Although fully saturated soil condition was not controlled by a B-value check in this test the close agreement between the measured SWRC and the one reported in Ghayoomi et al. (2016) (Suprunenko 2015 in

the figure) confirms the validity of the saturation and desaturation process, where B-value criteria for full saturation inside a triaxial system was satisfied. Additionally, the wetting path of the SWRC is also displayed, but not used in this investigation. The experimental data was then used to estimate van Genuchten fitting parameters (displayed in Table 1).

For each of the cyclic tests, after reaching the suction equilibrium in the specimen, displacement-controlled cyclic shear was applied using the hydraulic actuator and the corresponding measurements were recorded. The soils were tested under drained conditions by allowing the flow pump to maintain constant pore water pressure (or suction). Tests were conducted under two different conditions including: 1) specimens with the same cyclic shear strain amplitude and varying degrees of saturation (Series A) and 2) specimens with the same degree of saturation and varying cyclic shear strain amplitudes (Series B). Equilibrium suction was regained before the tests should consecutive tests be run on the same specimens. Each test was conducted for 5 cycles at frequency of 1 Hz. The shear strain amplitudes applied to the specimens were at 0.020, 0.032, and 0.40% for series A and 0.017, 0.023, 0.029, 0.034, 0.045, 0.050, and 0.055% for series B. As part of series A tests, dry, fully saturated, and partially saturated specimens with matric suctions of 4, 5, 6, 8, and 10 kPa were tested in this study. A summary of testing program is outlined in Table 2.

Data Analysis Methods

The vertical deformation of the soil specimen was used to monitor the change of the height, compression, and vertical strain, which is equal to the volumetric strain for the constant area in DSS. Given the initial and the change in height, the consolidation settlement after applying the confinement and the dynamic compression after the induced dynamic motion can be calculated. In addition, changes in the relative density

can be computed from these recordings. The normal and shear stresses were calculated by dividing the vertical and horizontal loads (readings from the vertical and horizontal load-cells) by the cross-sectional area of the sample, respectively. The axial and shear strains were calculated by dividing the deformations (recorded by the vertical LVDT and horizontal capacitance transducers) by the initial height of the specimen prior to loading. The tests were performed in a strain-controlled mode, so the maximum induced shear strain level stayed the same (only reversed in direction) while the shear stress was measured. The height was then adjusted in the calculation for the consecutive tests. Although the specimen height might change slightly after each cycle during a test the shear strain was calculate based on initial height of the specimen prior testing given the following reasons: 1) the vertical compression due to cycles was small enough that it would not change the shear strain should the height of the specimen updated after each cycle; 2) the hysteresis loops did not show a noticeable hardening or softening that may have been caused by the densification of pore water pressure rise, respectively; and 3) number of actual cyclic load was limited to avoid major compression.

Two system compliance issues were diagnosed and considered in the analysis. 1) Vibrational movement of the top table attached to the top of the specimen as a result of the dynamic base shear: The net horizontal movement of the specimen in shear was calculated by subtracting the movement of the top table (recorded by an additional independent LVDT) from the displacement measured at the bottom of the specimen (recorded by the capacitance transducer). 2) Frictional resistance of the system due to the interaction between the low friction Thomson ball slides and the bottom table and also the interactions between individual rings that confine the sample: The frictional response of the system was accounted by correlating the net movement of the specimen with the

amount of force needed to overcome the friction, which was measured by testing a water specimen. The frictional resistance was then subtracted from the horizontal force recorded from the soil response. For both compliance modifications calibrated correlations were developed and implemented to correct the results.

The hysteretic response of the soil subjected to horizontal shear was plotted using the corrected shear stress and shear strain data (after compliance issues were considered). The secant modulus and damping ratio were, then, calculated for cycles 2 – 4, and averaged. The first and the last cycles were set up in the program for the ramp up and down in actuator control system. An example of the hysteresis loops obtained from DSS is shown in Figure 8 where the reference lines are superimposed. The secant shear moduli were obtained by taking the slope of the line A-A' which marks the minimum and maximum shear strains and the corresponding shear stresses; while the damping ratio was calculated using Equation 12 (Das 1993).

$$\zeta = \frac{1}{2\pi} * \frac{Area \ of \ Hysteresis \ Loop}{Area of \ Triangle \ OAB \ and \ OA'B'}$$
 (10)

The consistency of the hysteresis loops between the cycles with no difference in the shape and overall slope verifies that the minimal changes in pore pressure during cycles (shown in Figure 9) did not lead to soil softening or modulus reduction while approximately constant suction was preserved. As in any other experiments, minor variations in controlled parameters might be expected. For example, in this system, the vertical pressure, soil relative density prior to cyclic shear, and the induced strain were the parameters that showed slight scatter. In order to avoid inconsistencies among the soil specimens, all the measured modulus and damping ratios were modified to a

reference relative density of 45%, a reference vertical stress of 50 kPa, and the target shear strain for each test, using the following equations.

$$\frac{G_{modified}}{G_{unmodified}} = \frac{\zeta_{unmodified}}{\zeta_{modified}} = \left(\frac{\sigma_{modified}}{\sigma_{unmodified}}\right)^{0.5} * \left(\frac{K_{2,modified}}{K_{2,unmodified}}\right)$$
(11)

These equations were derived according to the fundamental knowledge of soil dynamics and based on the correlation proposed by Seed and Idriss (1970) (i.e. Equation 4) and Oztoprak and Bolton (2013) (i.e. Equation 7). The first term, $\left(\frac{\sigma_{modified}}{\sigma_{unmodified}}\right)^{0.5}$, accounts for slight difference on the applied vertical stress (σ) on the specimen. The second term, $\left(\frac{K_{2,modified}}{K_{2,unmodified}}\right)$, considers the effect of small variability in initial relative density resulted from sample preparation and consolidation settlement and the effect of minor scatter on applied shear strain between the tests.

The pore water pressures recorded by DPT were employed to ensure that the target initial suction was achieved. In addition, since the cyclic tests were intended to be performed under drained condition, it was important to maintain a constant pore pressure and consequently constant effective stresses throughout the test. The measured pore pressures after the shear cycles and also the changes in pore pressure (or suction) are shown Figure 9 (a) and (b), respectively. The plots show very minimal variance in pore pressure in both saturated and unsaturated sands, which sometimes even fall under the error range of DPT (0.05 kPa). In addition, the figures clearly show a relatively higher increase of pore pressure in sands tested under higher shear strains.

EXPERIMENTAL RESULTS AND DISCUSSION

Dynamic Compression

The multistage compression response of the sample series B is presented in Figure 10. It should be noted that since the sides of the specimens are confined laterally, the axial strain would be equal to the volumetric strain. The results showed an approximate value of the threshold shear strain, i.e. the amount of shear strain necessary to induce compressional behavior in the sand, to be roughly between 0.017% and 0.023%. Additionally, this figure shows the effect of suction (degree of saturation) on the amount of axial strain experienced by the specimens at larger shear strains. Although testing was done for a small range of shear strains, the results indicated that the partially saturated soils compressed less than the dry or fully saturated specimens after a series of cyclic shear. In addition, by increasing the suction the compressive strain decreases, except in the tests with 10 kPa suction. This could be attributed to different mechanisms of deformations in suctions passed residual degree of saturation, where water-air-soil meniscus might be disconnected. In addition, a slightly lower compression in saturated specimens in comparison with the one in dry specimens might be associated with possible slight imperfection in saturation process.

Strain-Dependent Shear Modulus and Damping

As it can be seen in Table 2, the induced shear strain in the soil specimens in this study fell in a limited range (i.e. approximately between 0.02% to 0.06%). It was important to show that the current DSS system is capable of capturing the modulus degradation and damping changes over this shear strain range. The consistency of the obtained modulus reduction data regardless of the degree of saturation for such narrow range of shear strain would validate the performance of the DSS system after the modifications. However, tests with other ranges of strains would be possible by switching the spring system as described earlier. In series B, cyclic DSS tests were performed on specimens with the same degree

of saturation (suction) to investigate the effect of the induced strain on the shear modulus and damping. The results of the modified dynamic properties, G, and damping ratio for various suction levels are presented in Figures 11 and 12, respectively.

As previously discussed, larger imparted shear strains resulted in a softer soil response with lower shear modulus, shown in Figure 11. This trend is consistent for all the degrees of saturations indicating the success of the machine in capturing the modulus reduction behavior under suction-controlled condition. The results of the damping ratios of the B-series for various suction levels are shown in Figure 12. The data indicated a consistent pattern with what was observed in Figure 11, where larger shear strains resulted in softer soils with higher damping ratios. Although the general trends in damping fell in agreement with modulus reduction, the results are not as consistently uniform. This can be attributed to the complex and approximate nature of damping calculations from the DSS data. Similar partially inconsistent patterns in damping ratio measured in DSS have been also reported by other investigators (e.g., Jafarzadeh and Sadeghi 2011).

Effect of Matric Suction on Shear Modulus and Damping

In another series of DSS tests, i.e. series A, sand specimens with different degrees of saturation (suction) were tested under the same shear strain level. This series was intended to show the influence of suction on increasing the effective stress in soils and consequently affecting the modulus and damping. The vertical stress (confinement) was kept constant while the suction was increased from zero (in both dry and saturated specimens) up to 10 kPa passing the residual degree of saturation. The changes of shear modulus with the degree of saturation and suction are shown in Figure 13 (a) and (b), respectively. Due to the narrow range of suction in this fine sand, the data in Figure 13 (a) is mainly concentrated near the zero degree of saturation. Thus, showing the variation of

shear modulus with respect to the suction as in Figure 13 (b) will clarify the influence of the suction on the shear modulus. However, the data in Figure 13 (a) better highlight the clear increase in shear modulus of unsaturated soil comparing with both dry and fully saturated soils.

451

452

453

454

455

456

457

458

459

460

461

462

463

464

465

466

467

468

469

470

471

472

473

474

The shear modulus increased by raising the suction value or drying the saturated specimen on the drying path of SWRC. However, as expected, dry specimens approximately resulted in the same modulus as in saturated specimens. One can notice a slight drop in modulus of the soil in 10 kPa suction. This irregular trend is consistent with what was observed in Figure 10, which was possibly attributed to the shift in mechanisms in disconnected air-water-soil menisci. The presence of a peak modulus in partially saturated sand is in accordance with previously reported trends (e.g. Qian et al. 1991, Ghayoomi and McCartney 2011) and also the concept of suction tensile stress in sand (Lu et al. 2007). The approximate effect of the matric suction on the stiffness values was between 10% - 15% increase at smaller strains (A1) compared to the dry cases, while at larger applied shear strains (A₃), the contribution of the matric suctions was around 5%. This showed a less significant impact of suction in higher shear strains in cyclic DSS tests. Overall, this form of modulus variation is mostly in accordance with previously reported trends in small-strain shear modulus of unsaturated sand (e.g. Ghayoomi and McCartney 2011) and can be attributed to the expected suction stress pattern in unsaturated sand (Lu et al. 2007). Lu et al. (2010) explained that the stiffness and strength properties of soils are much better correlated with suction stress in comparison with matric suction. They showed that the suction stress reaches a peak by increasing the matric suction in sands as a result of different interaction mechanisms in air-water-solid interface system.

The increase in modulus due to higher suction values could have been predicted because of the influence of suction on the effective stress; i.e. partially saturated specimens were under higher effective stress, so they resulted in higher shear modulus. In theory, by normalizing the modified shear modulus values against the mean effective stress, the soils with the same relative density that experienced the same shear strain should result in the same shear modulus regardless of the degree of saturation. However, estimating an accurate effective stress in unsaturated soil is a challenging task even after an extensive amount of research on this topic in recent years. In order to investigate this theory, the obtained shear modulus values from A-series tests were normalized by the square root of the effective stresses ratio calculated for dry, saturated, and partially saturated soils, as in Equation 14; all for 50 kPa. The square root ratio was chosen based on the well-known empirical correlations between modulus and effective stress in sands.

$$G_N = G \sqrt{\frac{\sigma'_{dry}}{\sigma'_{unsaturated}}} \tag{12}$$

The normalized shear modulus (G_N) for different suction values are shown in Figures 14 (a) and (b), where the effective stresses were calculated using Equation 10 (Lu et al. 2010) and Equation 11 (Khalili and Khabbaz 1998), respectively. This normalization process clearly reduced the suction-induced increase in shear modulus. However, the extent of this reduction depends on the effective stress equation and the strain level. For example, applying the effective stress parameter proposed by Khalili and Khabbaz (1998) in Equation 11, resulted in less variability in shear modulus for various suction levels (i.e less increase in modulus due to the suction). In order to better present this difference, the ratio of the normalized shear moduli obtained using the two effective stress formulas (Equations 10 and 11) are shown in Figure 14 (c). This figure is basically the inverse of the

square root of the effective stress values calculated from these two equations. The slightly higher moduli resulted from the normalization based on the effective stress in Equation 10 (Lu et al. 2010) indicate a lower effective stress values predicted by this equation comparing with the ones by Equation 11.

In addition, larger induced shear strain reduced the significance of this modulus increase (e.g. when the soil was tested under 0.04% shear strain, where modulus stayed almost constant for various suction levels in Figure 14). In order to develop a unified approach, further experiments with wider range of strain and suction levels on soils with different mineralogy will be needed. However, the shear modulus relation might be different depending on the effective stress formula, strain level, and also testing method. For example, Ghayoomi et al. (2016) used a triaxial test or Khosravi et al. (2016) used resonant column test to show that still there would be meaningful increase in normalized modulus or constant effective stress modulus by increasing the suction or change of the degree of saturation. Considering the suction dependency of the shear modulus in addition to the previously known affecting parameters such as the effective stress, the void ratio, OCR, and the shear strain, an additional term could be included in available empirical relations to potentially account for the suction in estimating the shear modulus; hypothetical shown in Equation 15.

$$G = \left[A(OCR)^K f(e) \sigma_m^{\prime n} \right] [f(\gamma, \boldsymbol{\psi})] \tag{13}$$

where $[A(OCR)^K f(e) \sigma_m^{\prime n}]$ is the relation for G_{max} and $[f(\gamma, \psi)]$ is a suction- and strain-dependent function.

The changes of damping ratio with suction in tests series A are shown in Figure 15.

Overall, the damping ratio decreased by increasing the suction value or drying the saturated specimen on the drying path of SWRC. This signifies the stiffer response in

partially saturated sand specimens, although there is slight difference in damping ratio of specimens with different suction levels. However, the reduction in damping is not consistent between the tests with the different shear strain levels. As previously mentioned, this is due to the data scatter and uncertainties in calculating the damping ratio.

CONCLUSIONS

520

521

522

523

524

525

526

527

528

529

530

531

532

533

534

535

536

537

538

539

540

541

542

A custom built dynamic Direct Simple Shear (DSS) apparatus was modified for suctioncontrolled testing to study the effect of the degree of saturation on strain-dependent dynamic properties of unsaturated soils including shear modulus, damping, and dynamic compression. The results from the investigation confirmed the viability of the modified DSS to measure the suction-dependent dynamic properties of a clean sand even for a limited range of shear strain level. The shear modulus decreased consistently by increasing the induced shear strain regardless of the degree of saturation while the damping ratio increased. The results also showed that volumetric strains are smaller for partially saturated sand with larger matric suction values than those of dry or saturated sand when passing a certain shear strain threshold. Soils subjected to larger matric suctions were stiffer with higher shear modulus and lower damping where the peak moduli occur at about the start of the residual degree of saturation. The effect of matric suction on the dynamic shear modulus is more significant when tested under lower applied shear strains. Normalizing the shear modulus with respect to the effective stress reduced the impact of suction on modulus. However, the experimental results signified the suction-dependency of the shear modulus beyond the inclusion of the suction in the effective stress.

ACKNOWLEDGEMENT

- 544 The authors would like to acknowledge the partial funding of this project by the
- National Science Foundation through the NSF CMMI grant No. 1333810.
- 546 **REFERENCES**

- 547 Airey, D. W., and D. M. Wood. "An Evaluation of Direct Simple Shear Tests on
- 548 Clay." Géotechnique, 37(1), 1987, 25-35.
- 549 Alramahi, B., Alshibli, K. A., Fratta, D., and Trautwein, S., "A Suction-Control Apparatus
- for the Measurement of P and S-wave Velocity in Soils", ASTM Geotechnical Testing
- 551 Journal, 31(1), 2007, 1-12.
- 552 ASTM D6528-07, Standard Test Method for Consolidated Undrained Direct Simple Shear
- 553 Testing of Cohesive Soils, ASTM International, West Conshohocken, PA,
- 554 2007, www.astm.org.
- Bishop A.W., "The principle of effective stress", *Tek. Ukeblad*, 106(39), 1959, 859-863.
- 556 Cary, C. E., Zapata, C. E. 2016 "Pore Water Pressure Response of Soil Subjected to
- 557 Dynamic Loading under Saturated and Unsaturated Conditions", ASCE International
- Journal of Geomechanics, 1-9 (In Press).
- 559 Budhu, M., "Nonuniformities Imposed by Simple Shear Apparatus.", Canadian
- 560 Geotechnical Journal., 21(1), 1984, 125-37.
- 561 Craciun, O. and Lo, S.-C. R., "Matric Suction Measurement in Stress Path Cyclic Triaxial
- Testing of Unbound Granular Base Materials", ASTM Geotechnical Testing Journal,
- 563 33(1), 2010, 1-12.
- 564 Cui, Y.J., Tang, A.M., Marcial, D., Terpereau, J.M., Marchadier, G., and Boulay, X. "Use
- of a Differential Pressure Transducer for the Montoring of Soil Volume Change in

- 566 Cyclic Triaxial Test on Unsaturated Soils." ASTM Geotechnical Testing Journal,
- 567 30(3), 2007, 1-7.
- Darendeli, M. B. "Development of a new family of normalized modulus reduction and
- material damping curves." *PhD dissertation*, Univ. of Texas at Austin, Austin, Texas.
- 570 2001.
- Das, B. M., "Principles of Soil Dynamics", Boston: PWS-Kent Pub., 1993.
- 572 Dong, Y., McCartney, J. S., Lu, N. Small-Strain Shear Modulus Model for Saturated and
- 573 Unsaturated Soil. Go-Chicago, 2016, pp. 316-325.
- 574 Dunstan, A. H. "Laboratory Simulation of Earthquake Loading on Clay." MSc Thesis.
- University of New Hampshire, 1998. Print.
- 576 Ghayoomi, M. and McCartney, J.S. "Measurement of Small-Strain Shear Moduli of
- Partially Saturated Sand during Infiltration in a Geotechnical Centrifuge." ASTM
- 578 *Geotechnical Testing Journal*, 34(5), 2011, 1-12.
- 579 Ghayoomi M., McCartney, J.S., and Ko, H.-Y. "Empirical Methodology to Estimate
- Seismically Induced Settlement of Partially Saturated Sand", ASCE Journal of
- 581 Geotechnical and Geoenvironmental Engineering, 139(3), 2013, pp. 367-376.
- 582 Ghayoomi, M., Suprunenko, G., and Mirshekari, M. "Cyclic Triaxial Test to Measure
- 583 Strain-Dependent Shear Modulus of Unsaturated Sand", ASCE International Journal
- of Geomechanics, 2016. (Under Review).
- Hardin, B.O., Drnevich, V.P. "Shear Modulus and Damping in Soils: Design Equations
- and Curves.", J. Soil Mech. Found. Div. Proc. ASCE 98, No. SM7, 1972, 667–692.
- Hilf, J.W. "An Investigation of Pore-Water Pressure in Compacted Cohesive Soils", *Ph.D.*
- *Thesis*, University of Colorado, Boulder, 1956.

- 589 Hoyos, L.R., Suescun-Florez, E.A., and Puppala, A.J. "Stiffness of Intermediate
- 590 Unsaturated Soil from Simultaneous Suction-Controlled Resonant Column and
- bender Element Testing." Engineering Geology, 2015,188, 10-28.
- Jafarzadeh, F. and Sadeghi, H. "Experimental Study on Dynamic Properties of Sand with
- Emphasis on the Degree of Saturation." *Soil Dynamics and Earthquake Engineering*.
- 594 32(1), 2012, 26-41.
- Khalili, N., Khabbaz, M.H. "A unique relationship of chi for the determination of the shear
- strength of unsaturated soils." *Géotechnique*, 48(5), 1998, 681 687.
- 597 Khosravi, A., Ghayoomi, M., and McCartney, J.S. "Impact of effective stress on the
- dynamic shear modulus of unsaturated sand." *GeoFlorida*, West Palm Beach, Florida,
- 599 USA, 2010, 20-24.
- 600 Khosravi, A. and McCartney, J. S. "Resonant Column Test for Unsaturated Soils with
- Suction-Saturation Control." Geotechnical Testing Journal. 34 (6), 2011, 1 10.
- Khosravi, A., Shahbazan, P., and Pak, A., "Characterizing Variations in the Small Strain
- Shear Modulus of Unsaturated Sand during Hydraulic Hysteresis", Canadian
- 604 Geotechnical Journal, (Under Review).
- Kimoto, S., Oka, F., Fukutani, J., Yabuki, T., and Nakashima, K. "Monotonic and Cyclic
- Behavior of Unsaturated Sandy Soil under Drained and Fully Undrained Conditions."
- 607 Soils and Foundations, 51(4), 2011, 663-681.
- Kjellman, W. "Testing the Shear Strength of Clay in Sweden." Géotechnique. 2(3), 1951,
- 609 225-32.
- 610 Kramer, S.L. Geotechnical Earthquake Engineering. Prentice Hall, New Jersey. 1996.
- 611 Le K. "A Direct Simple Shear Device for Dynamic Characterization of Partially Satuarted
- Soils", Master Thesis, University of New Hampshire. 2016. Print.

- 613 Lu N. and Likos W.J., "Suction stress characteristic curve for unsaturated soil", Journal
- of Geotechnical and Geo-environmental Engineering, 132(2), 2006, 131-142.
- 615 Lu N., Wu, B., and Tan, C.P. "Tensile Strength Characteristics of Unsaturated Sands."
- ASCE Journal of Geotechnical and Geoenvironmnetal Engineering, 133(2), 2007,
- 617 144-154.
- 618 Lu, N., Godt, J.W., and Wu, D.T. "A Closed Form Equation for Effective Stress in
- Unsaturated Soil." Water Resources Research, 46, W05515, 2010, 14pp.
- 620 Mancuso, C., Vassallo, R., and d'Onofrio, A., "Small Strain Behavior of a Silty Sand in
- 621 Controlled-Suction Resonant Column-Torsional Shear Tests." Canadian
- 622 Geotechnical Journal. CGJ. 39(1), 2002, 22-31.
- Marinho, E.A.M., Chandler, R.J., and Crilly, M.S. 1995. "Stiffness Measurements on an
- Unsaturated High Plasticity Clay using Bender Elements." Proc. of the First
- International Conference on Unsaturated Soils, UNSAT '95, Paris, France, 6–8
- 626 September 1995. A.A. Balkema, Rotterdam, the Netherlands. Vol. 2. 535–539.
- Marinho, F.A.M., Take, W.A., and Tarantino A. "Measurement of Matric Suction Using
- Tensiometric and Axis Translation Techniques", Journal of Geotechnical and
- 629 Geological Engineering. 2008. Vol. 26. 615-631.
- 630 Mendoza, C.E., Colmenares, J.E., and Merchan, V.E., "Stiffness of an Unsaturated
- 631 Compacted Clayey Soil at Very Small Strains." Conf. on Advanced Experimental
- Unsaturated Soil Mechanics. Trento, Italy. 27-29 June. 2005, 199-204.
- Masing, G. "Eigenspannungen und Verfestgung Beim Masing," Proceedings, Second
- International Congress of Applied Mechanics, 1926. pp.332-335
- 635 Meng, F.-Y., "Dynamic Properties of Sandy and Gravelly Soils", *PhD Thesis*, The
- University of Texas at Austin, 2003.

- 637 Michaels P. "Comparison of viscous damping in unsaturated soils, compression and
- shear." Proc. Unsaturated soils 2006, Carefree, Arizona, 2006, 565-576.
- 639 Milatz, M., and Grabe, J. "A New Simple Shear Apparatus and Testing Method for
- Unsaturated Sands." *Geotechnical Testing Journal*. 38(1), 2015, 9-22.
- Miller, H.J. "Development of Instrumentation to Study the Effects of Aging on the Small
- Strain Behavior of Sands." PhD Dissertation, University of New Hampshire, 1994.
- 643 Print.
- Ng, C.W.W., Xu, J. and Yung, S.Y. "Effects of imbibition-drainage and stress ratio on
- anisotropic stiffness of an unsaturated soil at very small strains." Canadian
- 646 Geotechnical Journal, 46(9), 2009, 1062-1076.
- Oztoprak, S., and M.d. Bolton. "Stiffness of Sands through a Laboratory Test Database."
- 648 Géotechnique, 63(1), 2013, 54-70.
- 649 Qian, X., Gray, D.H., and Woods, R.D. "Resonant column tests on partially saturated
- 650 sands." *Geotechnical Testing Journal*. 14(3), 1991, 266–275.
- 651 Seed, H.B. and Idriss I.M. "Soil Moduli and Damping Factors for Dynamic Response
- Analyses." Rep. No. EERC70-10. Earthquake Eng. Res. Ctr., Univ. of California,
- 653 Berkeley, California. 1970.
- 654 Shen, C. K., Sadigh, K., and Herrmann, L. R., "An Analysis of NGI Simple Shear Apparatus
- for Cyclic Soil Testing," Dynamic Geotechnical Testing, ASTM STP 654, American
- Society for Testing and Materials, 1978, pp. 148 162.
- 657 Suprunenko, G. "Suction-Controlled Cyclic Triaxial Test to Measure Strain-Dependent
- Dynamic Shear Modulus of Unsaturated Sand". MSc Thesis. University of New
- Hampshire, 2015. Print.
- 660 Terzaghi, K. V. Theoretical Soil Mechanics. New York: Wiley, 1943. Print.

van Genuchten, M. A Closed Form Equation for Predicting the Hydraulic Conductivity of
 Unsaturated Soils." Soil Sci. Soc. Am. J., 58, 1980, 647-652.
 Wu, S., Gray, D.H., and Richart, Jr., F.E. "Capillary Effects on Dynamic Modulus of Sands
 and Silts", ASCE, Journal of Geotechnical Engineering, 110(9), 1984, 1188-1203.

List of Table and Figure Captions 666 667 668 Table 1. Physical and hydraulic properties of F-75 Ottawa sand 669 Table 2. DSS testing plan 670 671 672 Fig. 1: Cyclic hysteresis shear stress-strain relationship 673 **Fig. 2:** Shear modulus reduction function (after Kramer 1996) 674 Fig. 3: Modified DSS System Schematic view 675 Fig. 4: UNH – Cyclic Direct Simple Shear Apparatus 676 Fig. 5: DSS Soil Chamber schematic view 677 Fig. 6: Grain-size distribution for F-75 Ottawa Sand 678 Fig. 7: Soil-water retention curve for F75 Ottawa sand 679 Fig. 8: Example hysteresis loops (reference lines are added) 680 Fig. 9: (a) Measured pore water pressure (suction); (b) Changes of pore pressure after cycles of dynamic 681 shear 682 Fig. 10: Dynamic compression in dry, saturated, and partially saturated sand specimens 683 Fig. 11: Shear modulus reduction for various degrees of saturation 684 Fig. 12: Changes of damping ratio with shear strain for various degrees of saturation 685 Fig. 13. Effect of (a) degree of saturation; (b) matric suction on shear modulus of dry, saturated, and 686 unsaturated sand 687 Fig. 14. Effect of matric suction on effective stress-based normalized shear modulus of dry, saturated, and 688 unsaturated sand where the effective stress is calculated using (a) Equation 10 (Lu et al. 2010); (b) 689 Equation 11 (Khalili and Khabbaz 1998); (c) the ratio of the two normalized modulus 690 Fig. 15. Effect of matric suction on damping ratio of dry, saturated, and unsaturated sand

Table 1. Physical and hydraulic properties of F-75 Ottawa sand

<u>Input Parameter</u>	<u>Value</u>
Coefficient of curvature, C_c	1.83
Coefficient of uniformity, C_u	1.09
Specific gravity, G_s	2.65
D ₅₀ (mm)	0.182
Dry density limits, ρ_{d-min} , ρ_{d-max} (kg/m ³)	1469, 1781
Void ratio limits, e_{min} , e_{max}	0.486, 0.805
Relative density, D_r	0.45
Friction angle (deg) at $D_r = 0.45$	40
Poisson's ratio, v	0.38
van Genuchten's <i>a</i> parameter (kPa ⁻¹)	0.25
van Genuchten's N parameter	8
Residual Volumetric Water Content, θ_r	0.07
Saturated Volumetric Water Content, θ_s	0.39
	ı

Table 2. DSS testing plan

Sample Name	Applied Matric Suction (kPa)	Applied Normalized Shear Strain (%)
A1	0 (Dry, Saturated), 4, 8, 10	0.02
A2	0 (Dry, Saturated), 4, 8, 10	0.032
A3	0 (Dry, Saturated), 4, 8, 10	0.04
B1	0 (Dry)	0.023, 0.029, 0.035, 0.04, 0.045, 0.05, 0.055, 0.059
B2	0 (Saturated)	0.017, 0.023, 0.029, 0.035, 0.04, 0.045, 0.05, 0.055
В3	4	0.017, 0.023, 0.029, 0.035, 0.04, 0.045, 0.05, 0.055, 0.059
B4	5	0.017, 0.023, 0.029, 0.035, 0.04, 0.045, 0.05, 0.055
В5	6	0.017, 0.023, 0.029, 0.035, 0.05, 0.055, 0.059
В6	8	0.017, 0.023, 0.029, 0.035, 0.04, 0.045, 0.05, 0.055, 0.059
В7	10	0.017, 0.023, 0.029, 0.035, 0.04, 0.045, 0.05, 0.055, 0.059

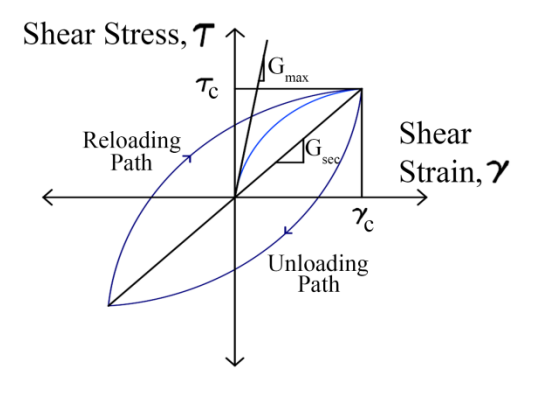


Fig. 1: Cyclic hysteresis shear stress-strain relationship

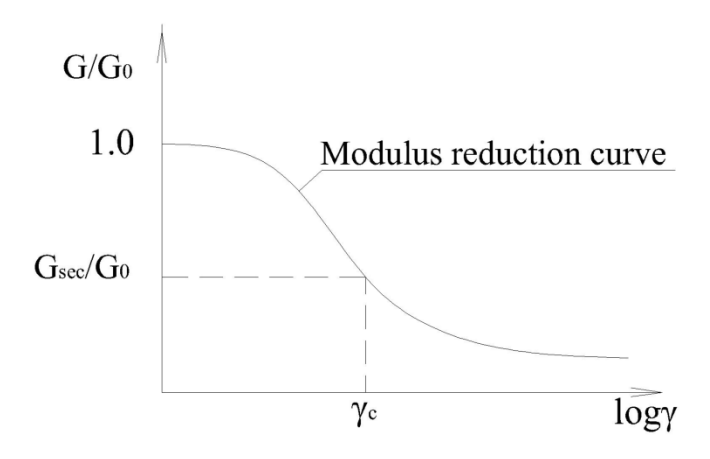


Fig. 2: Shear modulus reduction function (after Kramer 1996)

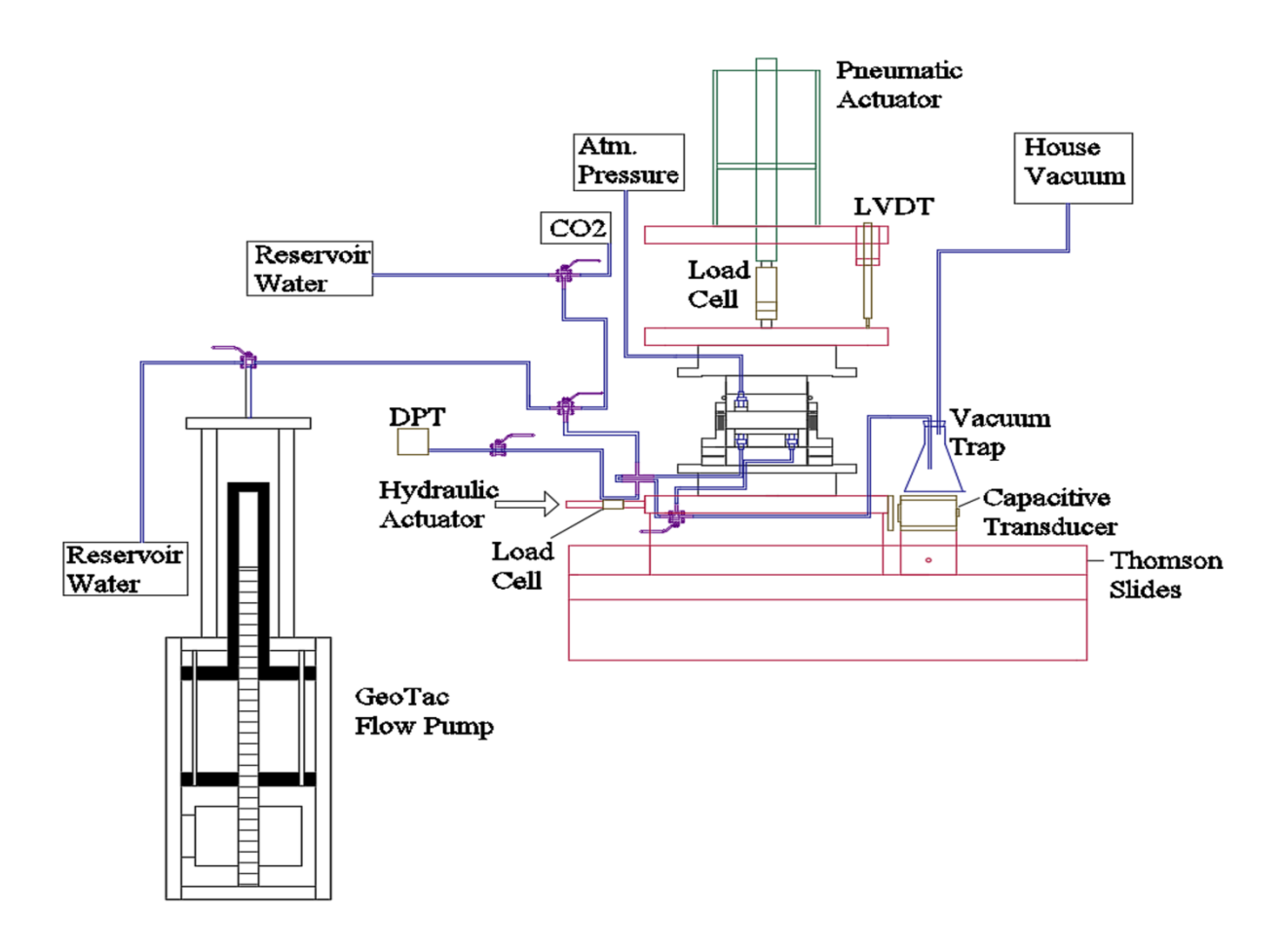


Fig. 3: Modified DSS System Schematic view

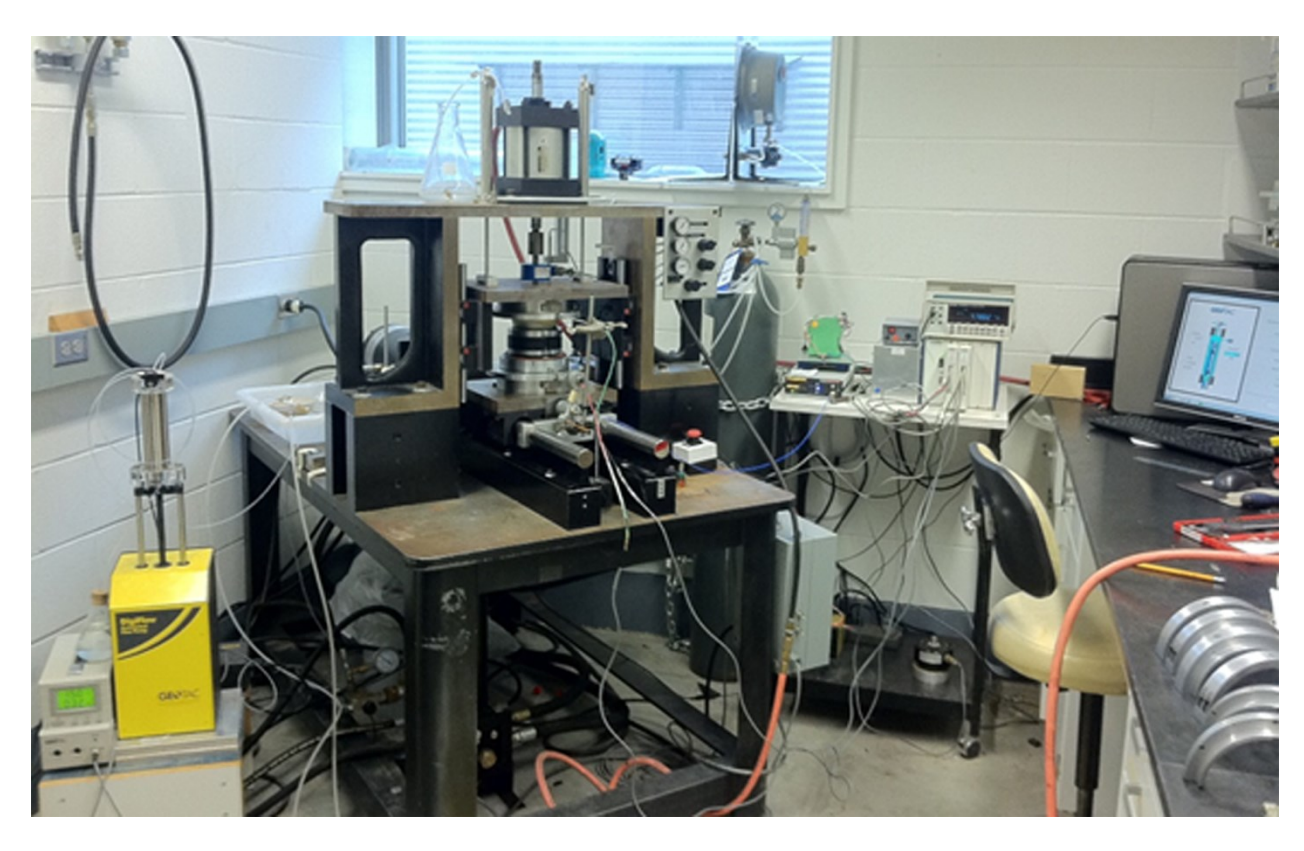


Fig.4: UNH – Cyclic Direct Simple Shear Apparatus

Top Platen

HAEV
Ceramic
Disk
Soil Specimen
Ring Stack
Water
Channel
Bottom
Platen

Fig. 5: DSS Soil Chamber schematic view

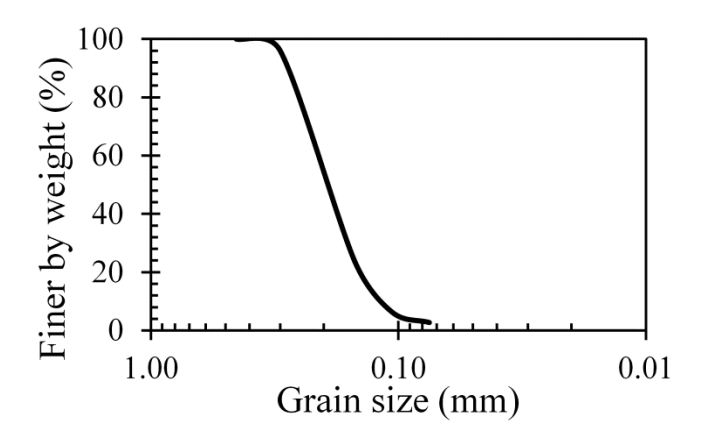


Fig. 6: Grain-size distribution for F-75 Ottawa Sand

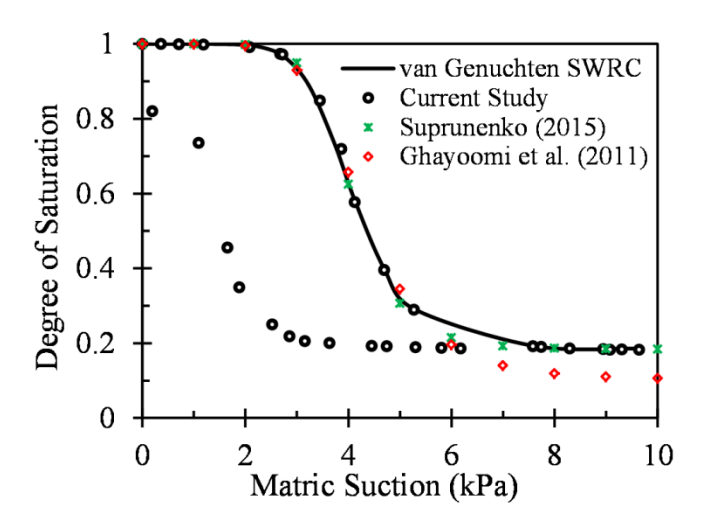


Fig. 7: Soil-water retention curve for F75 Ottawa sand

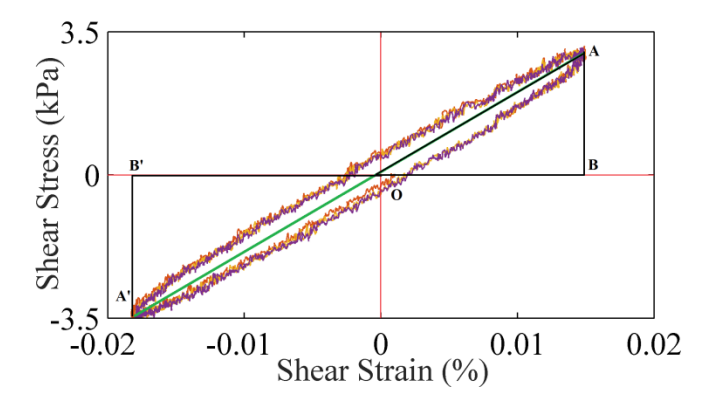


Fig. 8: Example hysteresis loops (reference lines are added)

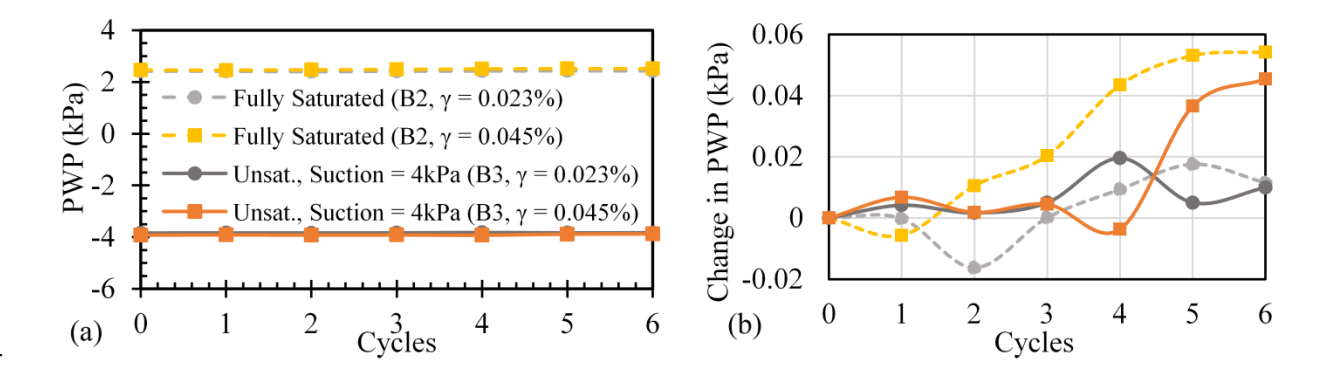


Fig. 9: (a) Measured pore water pressure (suction); (b) Changes of pore pressure after cycles of dynamic shear

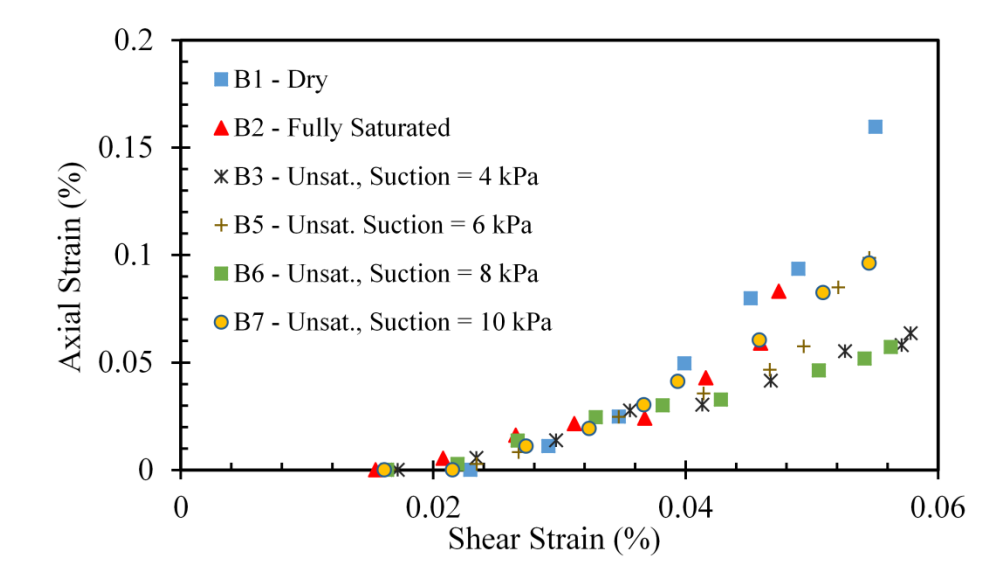


Fig. 10: Dynamic compression in dry, saturated, and partially saturated sand specimens

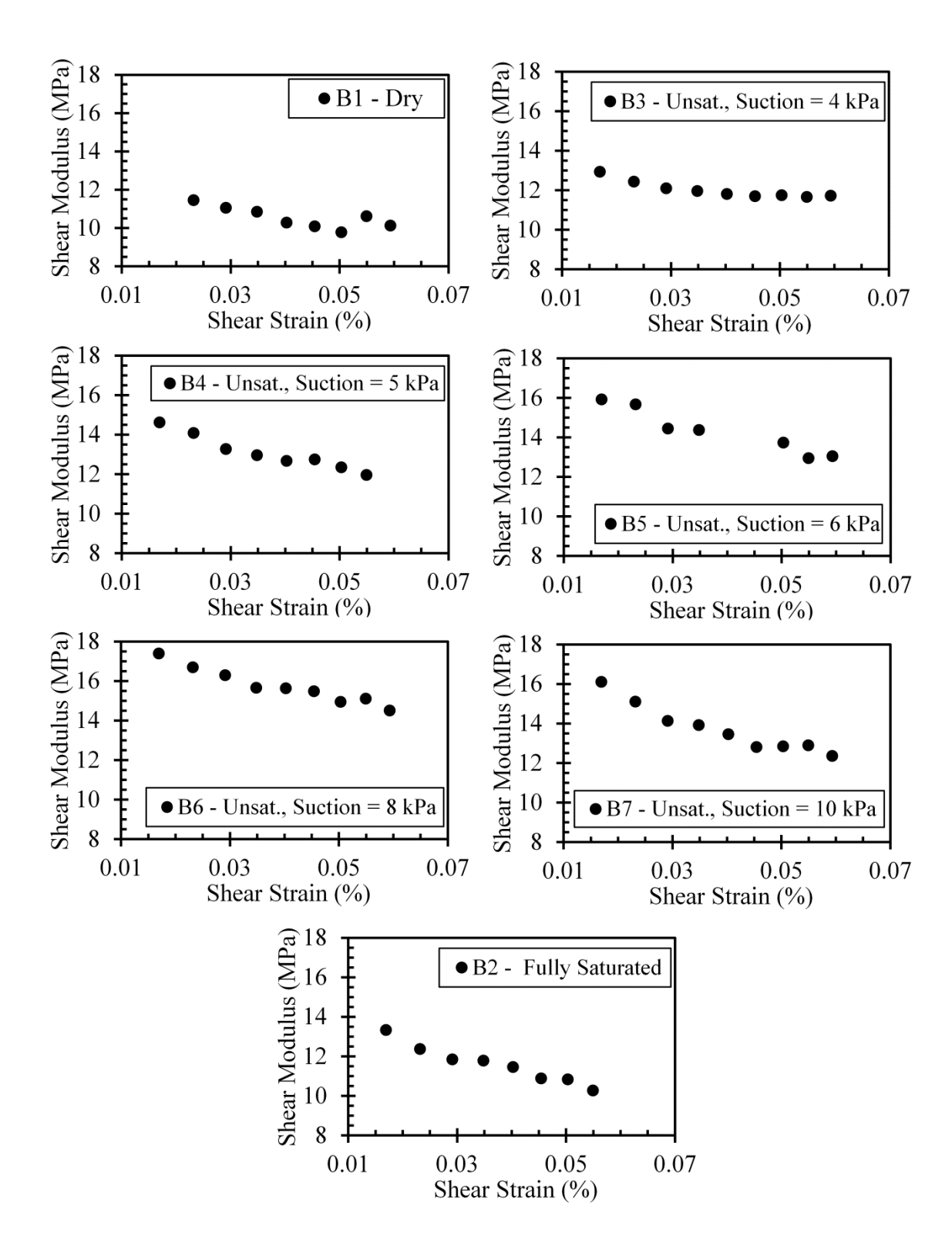


Fig. 11: Shear modulus reduction for various degrees of saturation.

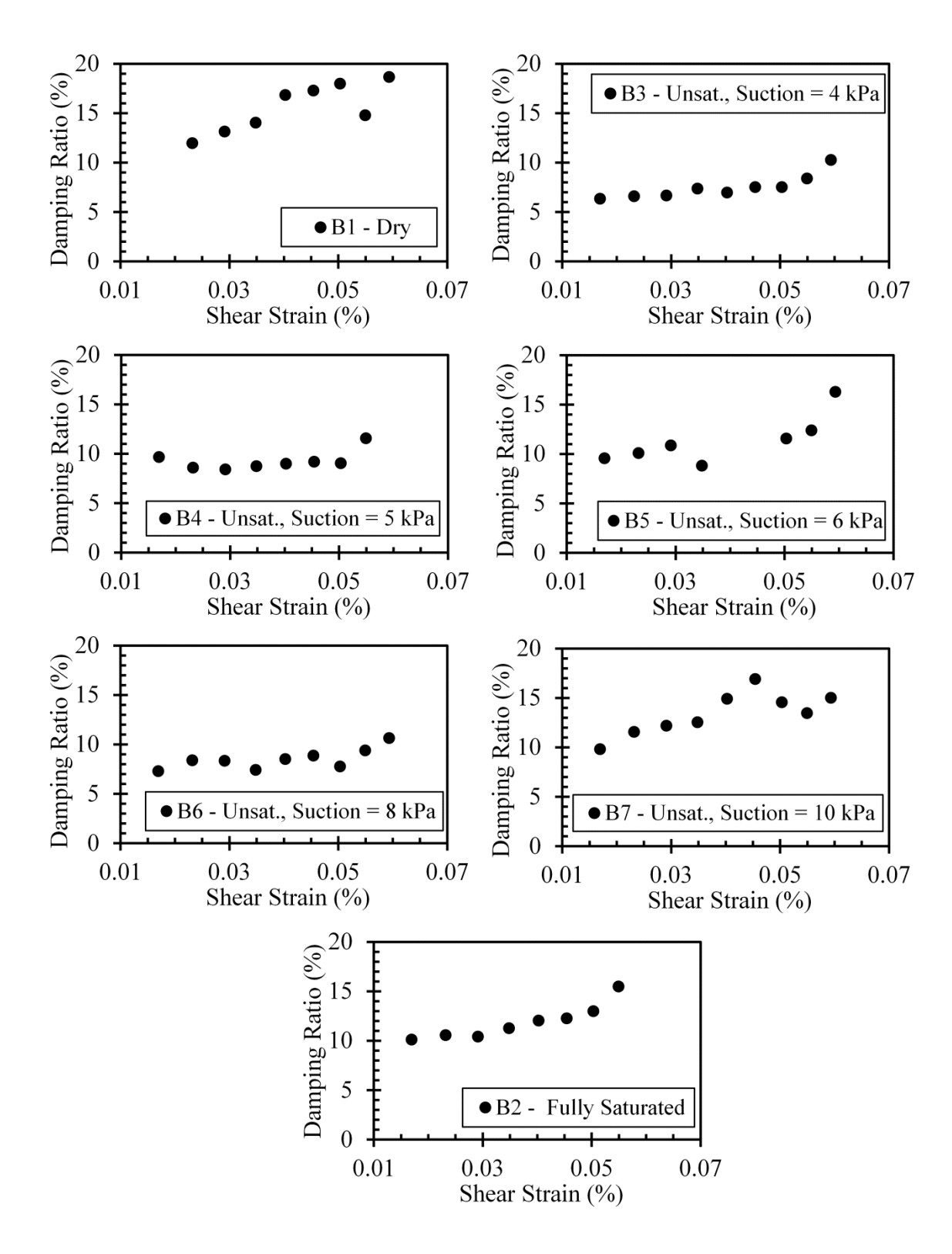


Fig. 12: Changes of damping ratio with shear strain for various degrees of saturation.

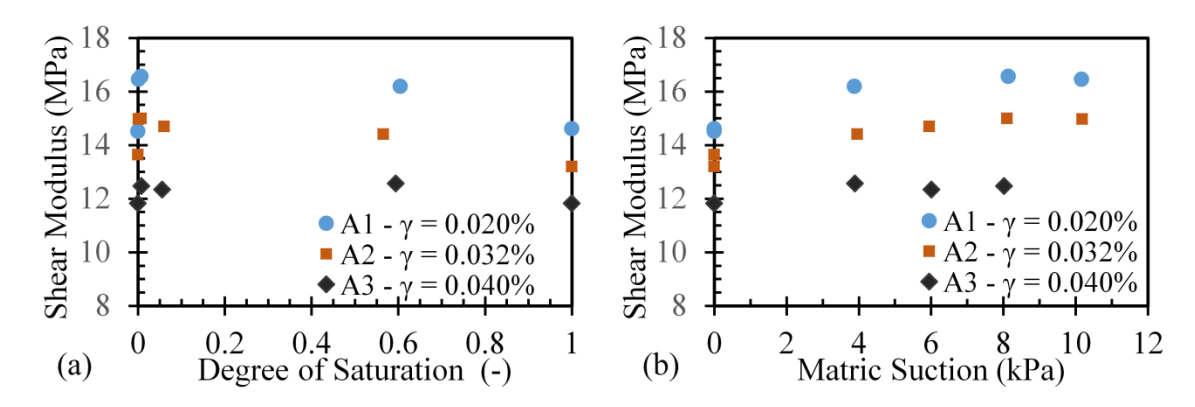


Fig. 13. Effect of (a) degree of saturation; (b) matric suction on shear modulus of dry, saturated, and unsaturated sand

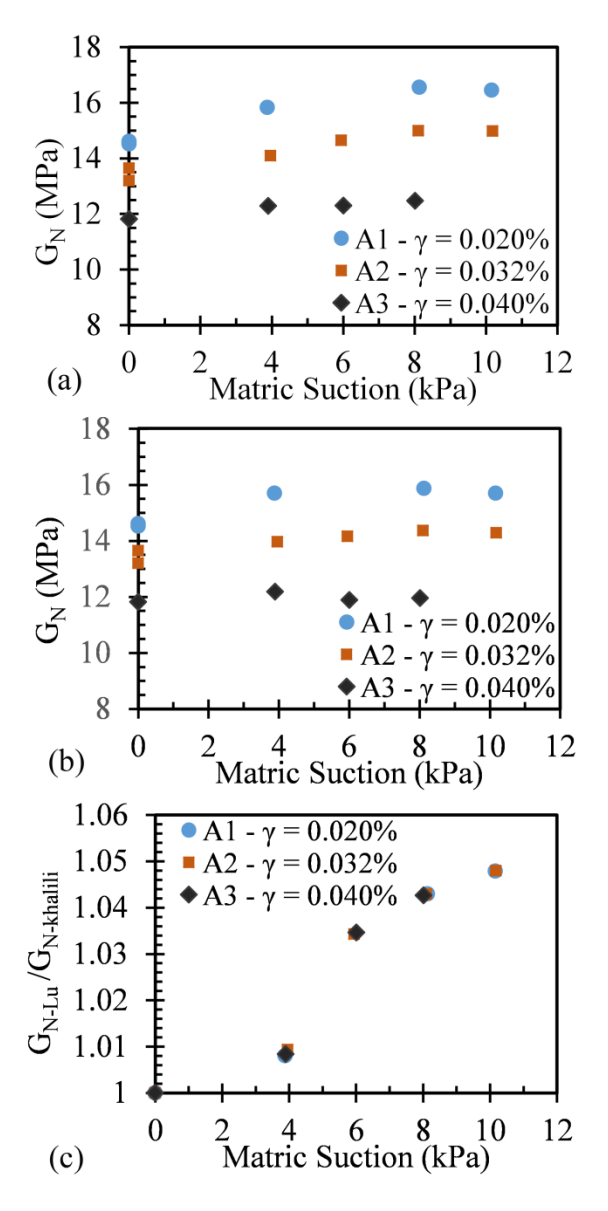


Fig. 14. Effect of matric suction on effective stress-based normalized shear modulus of dry, saturated, and unsaturated sand where the effective stress is calculated using (a) Equation 10 (Lu et al. 2010); (b) Equations 8 and 11 (Khalili and Khabbaz 1998); (c) the ratio of the two normalized modulus.

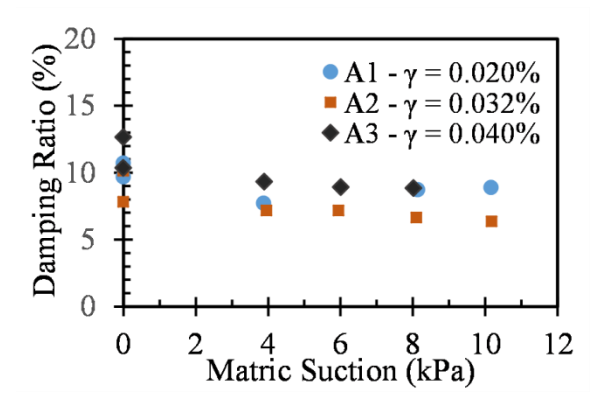


Fig. 15. Effect of matric suction on damping ratio of dry, saturated, and unsaturated sand